Earthquakes and Structures, *Vol. 5, No. 6 (2013) 753-779*
DOI: http://dx.doi.org/10.12989/eas.2013.5.6.753

Seismic collapse propagation in 6-story RC regular and irregular buildings

Somayyeh Karimiyan[*1], Abdolreza S. Moghadam[2a], Morteza Karimiyan[3b] and Ali Husseinzadeh Kashan[4c]

[1,2]International Institute of Earthquake Engineering and Seismology (IIEES), Tehran, Iran
[3]Applied Science and Technology University, Tehran, Iran
[4]Department of Industrial Engineering, Faculty of Engineering, Tarbiat Modares University, Tehran, Iran

(Received June 12, 2013, Revised September 9, 2013, Accepted September 13, 2013)

Abstract. One of the most important issues in progressive collapse mechanism of the buildings is evaluation of the collapse distribution in presence of the earthquake loads. Here, collapse propagation is investigated by tracking down the location and type of the collapsed beam and column elements, from the first element to the entire buildings. 6-story reinforced concrete ordinary moment resisting frame buildings with one directional mass eccentricity of 0%, 5%, 15% and 25% are studied to investigate differences among the progressive collapse mechanism of the regular and irregular buildings. According to the results of the nonlinear time history analyses, there are some patterns to predict progressive collapse scenarios in beam and column elements of the similar regular and irregular buildings. Results also show that collapse distribution patterns are approximately independent of the earthquake records.

Keywords: irregular buildings; collapse distribution; progressive collapse; reinforced concrete buildings; earthquake load

1. Introduction

Progressive collapse mechanism in a structure means the collapse of a major portion or the entire building which is initiated by the propagation of local damages in such a way that the structural system cannot bear the main structural loads. In this mechanism, the final damage state is much more than the initial local damages (Ellingwood 2006).Vehicular collision, accidental overload, aircraft impact, design/construction error, fire, gas explosions, bomb explosions, hazardous materials, etc are as a number of abnormal loads which can potentially be the trigger of progressive collapse in the various buildings (Somes 1973, Burnett 1975a).

According to the current design specifications, computationally macro models of 2D ten-story steel moment resisting frames were seismically designed for high and moderate seismic risks have been developed to compare progressive collapse mechanism using beam and column finite-element

[*]Corresponding author, Ph.D., E-mail: s.karimiyan@iiees.ac.ir
[a] Assistant Professor, E-mail: moghadam@iiees.ac.ir
[b] M.Sc., E-mail: info@karimiyan.com
[c] Assistant Professor., E-mail: a.kashan@modares.ac.ir

http://www.techno-press.org/?journal=eas&subpage=7 ISSN: 2092-7614 (Print), 2092-7622 (Online)

models. Results of the simulation demonstrated that the progressive collapse potential of the frames which were designed for moderate seismic risk, is more than those designed for high seismic risk. To have a better resistance to progressive collapse, system strength is more effective than the improved ductile detailing in the structural systems and the alternate path method was also illustrated as a useful method against the progressive collapse mechanism (Khandelwal *et al.* 2012).

The macro model-based simulation method was also used in 2D reinforced concrete moment resisting frames which were designed for lateral load requirements in seismic and non seismic regions. Results demonstrated that designing based on the high seismicity zone provisions and using special RC moment frame in buildings are more effective than RC frame structures designed for low or moderate seismic risk in progressive collapse evaluation. Using a macro model-based approach is viable to investigate progressive collapse potential of the buildings (Bao *et al.* 2012).

One of the most frequently used procedures for resistance to progressive collapse has shown the alternate path method. Evaluation of the overall stability of moment-resisting (sway) frames and nonsway frames which include lateral-force resisting elements showed that considering the global response of the damaged structures is necessary for assessment of progressive collapse, also demonstrated that the progressive collapse investigations should be applied to seismic and direct blast hazards (Ettouney *et al.* 2012).

Collapse mechanisms and earthquake resistance to progressive collapse were investigated by Gurley (2012) via comparing sway collapse mechanisms in earthquake engineering and double-span mechanisms of GSA (2003) under explosion loads (columns removal). Based on the results, since earthquake damages can also remove the load bearing elements similar to the explosion loads, assessment of progressive collapse in the presence of earthquake loads is vital for designing against the progressive collapse. Investigation of the ductile detailing for the lost column events relevant to the specific collapse mechanisms showed that design according to earthquake engineering is a valuable approach for designing against the progressive collapse and it needs to include the “double span” mechanisms at lost columns.

Progressive collapse mechanism of RC frame structures were studied with assessment of two typical non-integrated slab and integrated cast-in-situ slab with different levels of seismic fortifications (Yi *et al.* 2011). Then the alternate path (AP) method was evaluated by investigation of the results of nonlinear dynamic analyses.

The progressive collapse simulation of 12-story, 3-bay precast panel shear wall in the presence of earthquakes loads were investigated by Pekau and Cui (2005) through a distinct element method (DEM) program. Integrity analyses were performed and shear ductility demands of the mechanical connectors in the vertical joints were investigated. Simulation of the progressive collapse processes of the panel wall in various conditions illustrated that if precast panel shear wall satisfies the seismic requirements, it will automatically provide the demands of shear ductility in vertical joints and shear slip in horizontal joints of connectors in progressive collapse assessment.

The relationship between earthquake-resistant reinforced concrete structures and progressive collapse mechanism were studied by Tsai and Lin (2008) according to GSA guidelines. Linear static, nonlinear static and nonlinear dynamic analyses were performed in the structures subjected to the columns removal. Results showed that because of the different collapse resistances, GSA criteria should be different for the two different nonlinear analyses and a dynamic amplification factor (DAF) of 2 causes the nonlinear static method to be conservative. Also it is required to consider DAF in the inelastic dynamic effects of GSA linear procedure. Nonlinear static capacity curve showed that it is possible to predict DAF and progressive collapse resistance in the column-removed RC buildings (Tsai and Lin 2008).

Three databases on experimental data of reinforced concrete beams, steel W-beams and tubular hollow square steel columns were developed to simulate the dynamic response until the collapse of the buildings. These databases were used to quantify important parameters which affect the cyclic moment-rotation relationship at plastic hinge regions in the steel and RC components subject to the earthquake loads. The application of these databases in the field of performance-based earthquake engineering has been illustrated via a study of a 4-story steel structure. Results showed that its seismic performance was successfully assessed in collapse evaluation of the building (Lignos and Krawinkler 2012 and 2013).

Plastic hinges which were defined according to FEMA-356 and those defined based on the properties of reinforced concrete members were compared with each other by Eslami and Ronagh (2012) in an eight-story and two four-story buildings with various ductilities. According to the results, FEMA-356 lumped hinges underestimate the strength and the displacement capacity of the buildings with low ductility frames.

Biskinis and Fardis (2009) developed a number of models according to the results of the experimental databases in reinforced concrete members to calculate the ultimate deformation, moment-rotation and secant stiffness at flexural yielding in RC elements. Explicit and simple expressions were presented which are free from the analysis of moment-curvature. Results showed that these models are valuable and helpful for the seismic evaluation and retrofitting of the reinforced concrete structures.

Based on the results of RC experimental tests and properties of the members, a number of mathematical expressions were developed by Panagiotakos and Fardis (2009) to calculate deformations at yielding and failure in reinforced concrete elements. However, results of the curvature expressions are considerably scattered in comparison with the results of the RC experimental tests.

Most of research works in the context of progressive collapse have studied column removal under explosion loads or collisions. (Helmy *et al.* 2012, Hayes Jr *et al.* 2012, Masoero *et al.* 2010, Khandelwala *et al.* 2009, Talaat and Mosalam 2009, Sasani and Kropelnicki 2008, Sasani and Sagiroglu 2008, Sasani and Sagiroglu 2008, Sasani *et al.* 2007, El-Tawil *et al.* 2007, Bažant and Verdure 2007, Lew 2003, Kaewkulchai and Williamson 2003, Karbassi and Nollet 2013, Stinger and Orton 2013, Orton and Kirby 2013, Hafez *et al.* 2013, Nateghi and Parsaeifard 2013).

However, there are a few researches that have considered the 3D progressive collapse of the buildings under earthquake loads and torsion effects. In 2011, rotational friction dampers were investigated against the earthquake loads and progressive collapse resisting capacities (Kim *et al.* 2011).

Progressive collapse mechanism in symmetric and asymmetric buildings was evaluated as a result of columns removal through designing 30-story regular and irregular structural models once with braced cores and once more with reinforced concrete cores. The results of analyzing the irregular structural models have shown that variation of the progressive collapse resisting capacities, were based on the location of removed columns. Progressive collapse potential of the irregular structure was increased, when the location of the removed column was determined in the tilted side of the building. The plastic hinges formed in the removed column bays and adjacent bays showed that other elements in the structural system were involved in resisting progressive collapse and when a structural member was removed, other elements contributed to resist against the progressive collapse. So, progressive collapse potentials of the asymmetric buildings were not very large in comparison with those of the corresponding symmetric buildings (Kim and Hong 2011).

Planar models in comparison with the 3D models were studied in 2011 with different assumptions in model simulations (Alashker *et al.* 2011). A few 10-story steel buildings, seismically designed in planar and 3D macro models, were considered to investigate the 2D and full 3D structural systems due to forcibly columns removal. Four different types of models were used to examine the various simulation approaches in progressive collapse assessments. Results showed that floor systems have significant effects on the distribution of the collapse response in 3D macro models. Therefore, because of the floor system contribution effects, 3D models were conservative and valuable in progressive collapse evaluation in comparison with the planar models.

Progressive collapse numerical simulation in reinforced concrete (RC) frames and RC shear-walls in presence of the earthquake loads were done using multi-layer-shell-element and fiber-beam-element models (Lu *et al.* 2008 and 2013). Nonlinear behavior of RC structural elements were simulated including the cyclic behavior under coupled axial force-bending moment and shear force, breakdown of the structural elements at ultimate states and contact between the structural elements during the collapse (Lu *et al.* 2008 and 2011).

Although there are many cases of the collapsed buildings in past earthquake events, usually the spread of collapse is not considered explicitly in seismic design or evaluation of the buildings. In this research the spread of collapse in the building subjected to the earthquake records is studied by continuing nonlinear time history analyses (NLTHA) even if some elements pass their collapse limit states.

Past earthquakes have shown that torsion in asymmetric plan buildings usually causes concentration of damage in one side of those buildings. Therefore it is expected that asymmetry in a building increases the progressive collapse potential of the building. In the present study, to evaluate the effect of asymmetry on the seismic progressive collapse potential of mid rise buildings, a set of regular and irregular 6-story ordinary moment resisting frame RC buildings are considered. At first, a regular building is designed based on ACI (2005), and then by introducing mass eccentricities of 5%, 15%, and 25% in the symmetric structural model, asymmetric version of the model buildings are created. Then, they are analyzed using a set of 2-component earthquake records.

As addressed in the paper, the aim of this study is to evaluate potential of the progressive collapse in the regular and irregular buildings. On the other hand, the probability of collapse in a building which is designed with ordinary moment resisting frames is higher than those with special or moderate moment resisting frames. As, there are many weak and traditional buildings in most countries, the building models with ordinary moment resisting frame are more important to be evaluated in terms of potential of the progressive collapse in comparison with the other building types.

6-story buildings are the target buildings in this research which are used in most countries as commercial, office and residential buildings. This may call for presenting useful and valuable criteria to investigate the progressive collapse mechanism of the mid rise reinforced concrete buildings.

2. The reference building

The models considered in this research are 6-story symmetric and asymmetric RC ordinary moment resisting frame buildings. These models have 3 bays with span of 5 m center to center in two directions X and Z. Height of the stories is 3.5 m. The design dead load and live load are 5.3 kN/m2 and 1.96 KN/m2 respectively. Fig. 1 shows 3D view of the building model.

The asymmetric building models are derived from the symmetric model via changing the mass distribution in such a way that an equal one way mass eccentricity being produced in the X direction of the all floors. The mass in each floor is distributed equally among the frame nodes in a symmetric building. In asymmetric buildings mass has been distributed in nodes of the frames in such a way that the value of lumped mass for the two left side frames are more than those in two right side frames.

Therefore, four building models with 0%, 5%, 15% and 25% mass eccentricities are studied in this research. The level of 25% mass eccentricity is considered to include the extreme amount of irregularity in the buildings. Because, there are a few special structures that have a mass eccentricity level more than 25%.

The farthest edge and the closest edge to the mass center are defined here as the stiff edge and the flexible edge, respectively. It is worth to mention that the effects of infills are not considered and rigid diaphragm assumption has been made in this study. The floor is considered in this study as a rigid in plane of slab. It is common to use the rigid slab assumption in the torsional buildings researches. The effect of the floor slabs is considered in determining stiffness of the beams. Moreover, our study is consistent with those studies are using 2 dimensional models. For example, please see the benchmark study of Haselton 2007 (FEMA P695 2009, Haselton and Deierlein 2007, Haselton *et al.* 2007, Haselton *et al.* 2008, Lignos and Krawinkler 2012, 2013).

Capacity curves from the pushover analyses and the periods of vibration for 4 regular and irregular buildings with the mass eccentricity of 5%, 15% and 25% are derived and shown in Fig. 2 and Table 1. The buildings have been pushed perpendicular to the mass eccentricity direction (in Z direction).

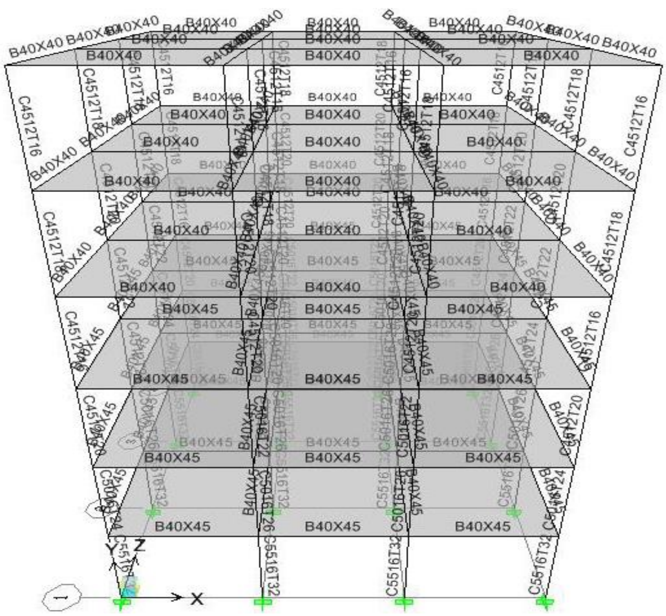

Fig. 1 3D view of the building model

Table 1 The periods of the buildings structural models (sec)

Mass	T1	T2	T3	T4	T5	T6	T7	T8	T9	T10
%0	1.44	1.345	1.24	0.5	0.498	0.42	0.26	0.255	0.218	0.16
%5	1.5	1.4	1.27	0.5	0.498	0.41	0.26	0.256	0.214	0.162
%15	1.607	1.485	1.105	0.533	0.5	0.365	0.27	0.26	0.191	0.175
%25	1. 59	1.45	0.93	0.55	0.5	0.3	0.29	0.255	0.187	0.159

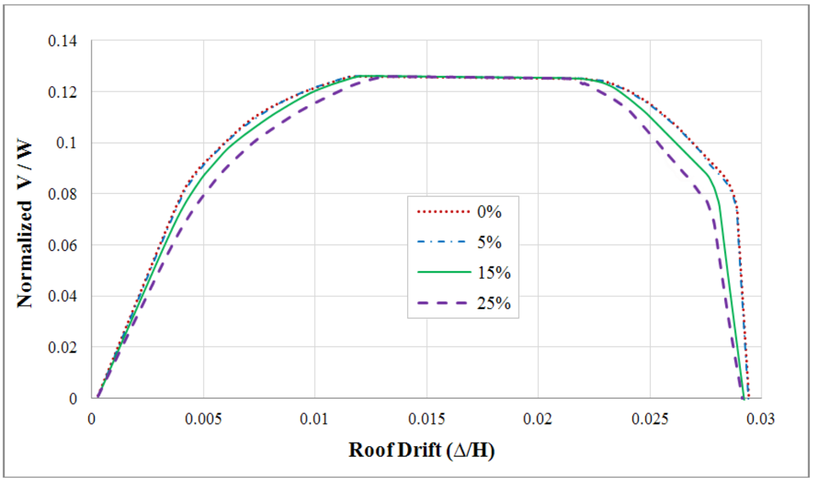

Fig. 2 Pushover curves for regular and irregular buildings with the mass eccentricity of 5%, 15% and 25%

It has been shown that careful selection of the element backbone curves is essential for a proper simulation of progressive collapse in buildings (FEMA P695 2009). Calibrated beam-column element model, which has been developed by Ibarra, Medina and Krawinkler (2005), is capable for collapse studies of RC frame buildings, globally. Fig. 3 shows Backbone curve of the modified Ibarra-Krawinkler model, and its associated definitions (for more details on the notations used in Fig. 3, please refer to the Appendix). This model includes the main aspects of the capping point, where monotonic strength loss begins, and the post-capping negative stiffness. These features enable us to model the strain-softening behavior associated with concrete crushing, rebar buckling and fracture, or bond failure (FEMA P695 2009).

In general, accurate simulation of side-sway structural collapse depends on the proper modeling of post-capping behavior. Researchers have also used a variety of methods to simulate cyclic response of reinforced concrete beam-columns, e.g., creating fiber models that can capture cracking behavior and the spread of plasticity throughout the element (Filippou 1999). The decision to use a lumped-plasticity approach was based on this observation that available fiber element models were not capable of simulating the strain-softening associated with rebar buckling, and thus could not reliably simulate the collapse of flexural dominated reinforced concrete frames (Ibarra and Krawinkler 2005, Haselton *et al.* 2007, FEMA P695 2009).

In this paper, the nonlinear behavior is represented using the concentrated plasticity in rotational springs. The rotational behavior of the plastic regions is according to the Modified Ibarra, Medina and Krawinkler Deterioration Model (Ibarra *et al.* 2005, Lignos and Krawinkler 2012, 2013).

The input parameters for the rotational behavior of the plastic hinges in models are determined

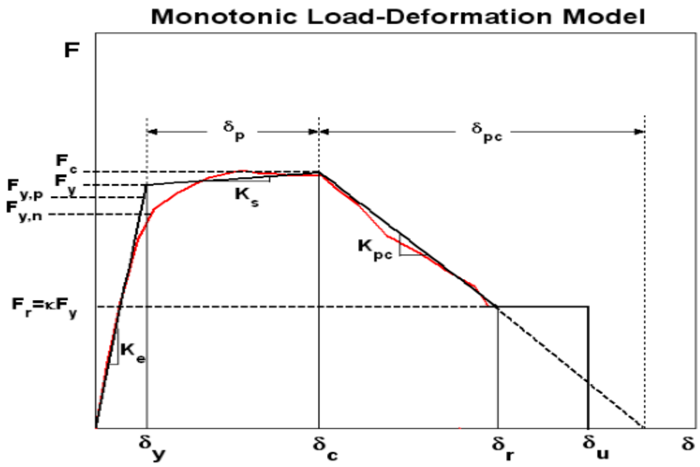

Fig. 3 Backbone curve of modified Ibarra-Krawinkler model and its associated definitions (Ibarra *et al.* 2004 and 2005, Lignos 2008, Lignos *et al.* 2008, Krawinkler *et al.* 2009, Haselton *et al.* 2009)

using empirical relationships developed by Lignos and Krawinkler (2012 and 2013) which have been derived from an extensive database of RC component tests. Alternately, these input parameters can be determined using approaches similar to those described in FEMA P695 (2009) and Haselton and Deierlein (2007).

Moment resisting frames are modeled with elastic beam-column elements connected by zero length elements which serve as rotational springs to represent the structure nonlinear behavior. As mentioned before, the springs follow a hysteretic response based on the Modified Ibarra, Medina and Krawinkler deterioration model. The effect of the plastic hinge length is considered in calculation of rotational behavior of the plastic hinges empirically from the test data (Haselton *et al.* 2007, FEMA P695 2009, Lignos and Krawinkler 2012, 2013, Panagiotakos and Fardis 2009, Biskinis and Fardis 2009, Karimiyan and Moghadam 2013).

According to Fig. 3, to simulate structural collapse, the parameter κ should be equal to zero. Also, based on the modified Ibarra-Krawinkler model shown in Fig. 4, zero strength is corresponded to the value of Θu. It means that, as soon as the value of Θ reaches to Θu, hinge strength would be equal to zero and hence the element is effectively eliminated from the structure. In other words, during NLTHA, when the value of Θ for a hinge reaches to its calculated value of Θu, the relevant beam or column element is removed from the structural system automatically and NLTHA is continued till the structural system becomes unstable. It is worth mentioning that Θu is calculated for each hinge according to the modified Ibarra-Krawinkler element model, and is inputted in Opensees structural models. In this study a hinge is considered as a collapsed one if its rotation exceeds the extreme value of Θu.

Deteriorating parameters have been used for the modified Ibarra-Krawinkler hysteretic model for modeling plastic hinges. There are comprehensive relationships for modeling deterioration parameters of the plastic hinges. These relationships were proposed through the calibration of several hundreds of experimental tests that associate available deterioration modeling parameters with section properties and detailing criteria that control deterioration in structural components. These relationships and related parameters were explained completely in Lignos and Krawinkler (2012 and 2013), FEMA P695 (2009), and Haselton and Deierlein (2007).

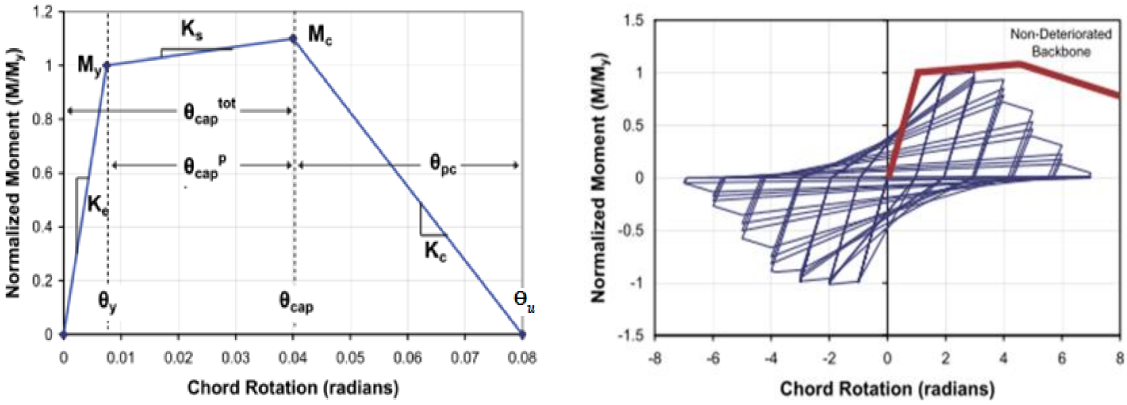

Fig. 4 Monotonic and cyclic behavior of component model used in this study (Ibarra and Krawinkler 2005, Haselton *et al*. 2007 and 2008, FEMA P695 2009, Zareian *et al*. 2009 and 2010)

Table 2 Summary of the used PEER NGA Database information and parameters of recorded ground motions for the far-Field record set (FEMA P695 2009)

ID No.	PEER-NGA Record information				Recorded motions	
	Records Seq. No.	Lowest Freq (Hz.)	File names – Horizontal record		PGA max (g)	PGV max (cm/s.)
			Component 1	Component 2		
1	953	0.25	NORTHR/MUL009	NORTHR/MUL279	0.52	63
2	960	0.13	NORTHR/LOS000	NORTHR/LOS270	0.48	45
3	1602	0.06	DUZCE/BOL000	DUZCE/BOL090	0.82	62
4	1787	0.04	HECTOR/HEC000	HECTOR/HEC090	0.34	42
5	169	0.06	IMPVALL/H-DLT262	IMPVALL/H-DLT352	0.35	33
6	174	0.25	IMPVALL/H-E11140	IMPVALL/H-E11230	0.38	42
7	1111	0.13	KOBE/NIS000	KOBE/NIS090	0.51	37
8	1116	0.13	KOBE/SHI000	KOBE/SHI090	0.24	38
9	1158	0.24	KOCAELI/DZC180	KOCAELI/DZC270	0.36	59
10	1148	0.09	KOCAELI/ARC000	KOCAELI/ARC090	0.22	40
11	900	0.07	LANDERS/YER270	LANDERS/YER360	0.24	52
12	848	0.13	LANDERS/CLW-LN	LANDERS/CLW-TR	0.42	42
13	752	0.13	LOMAP/CAP000	LOMAP/CAP090	0.53	35
14	767	0.13	LOMAP/G03000	LOMAP/G03090	0.56	45
15	1633	0.13	MANJIL/ABBAR--L	MANJIL/ABBAR—T	0.51	54
16	721	0.13	SUPERST/B-ICC000	SUPERST/B-ICC090	0.36	46
17	725	0.25	SUPERST/B-POE270	SUPERST/B-POE360	0.45	36
18	829	0.07	CAPEMEND/RIO270	CAPEMEND/RIO360	0.55	44
19	1244	0.05	CHICHI/CHY101-E	CHICHI/CHY101-N	0.44	115
20	1485	0.05	CHICHI/TCU045-E	CHICHI/TCU045-N	0.51	39
21	68	0.25	SFERN/PEL090	SFERN/PEL180	0.21	19
22	125	0.13	FRIULI/A-TMZ000	FRIULI/A-TMZ270	0.35	31

According to FEMA P695 (2009), Haselton (2007 and 2008) and Lignos and Krawinkler (2012 and 2013), the modified Ibarra-Krawinkler model does not directly consider the effect of axial-flexural interaction in the columns. This model considers the effect of constant moment in accordance with the specified axial load due to the existing loads. Such a modeling has been used in the mentioned references and they have recommended this method to simulate structural collapse. The models used in these researches are all 2 dimensional and the main purpose of our study is to extend their studies to 3 dimensional models.

Therefore, all of assumptions of these 2 dimensional models were considered also in our 3 dimensional models. In this way, the mentioned references form the base of control and comparison of the results in our research.

Also, currently available steel material models are not able to replicate the behavior of rebar as it buckles and fractures. Due to this limitation, current fiber models were judged inadequate for simulating collapse in RC and steel buildings. We hope that this modeling limitation being overcame in near future (Ibarra *et al.* 2005, Haselton and Deierlein 2007, Haselton *et al.* 2007 and FEMA P695 2009). So, the researchers have concluded that although the fiber element models consider the effect of axial-flexural interaction, they are not convenient to simulate the structural collapse. Based on the current comprehensive researches the modified Ibarra, Medina and Krawinkler deterioration model is the only element model to simulate the structural collapse.

2-component earthquake records are used to perform NLTHA based on FEMA P695 (Table A-4C), as shown in Table 2. Both components are applied on the structures in two horizontal directions X and Z in such a way that the Z components are stronger than X components in all earthquake records. Two hinges are considered at both ends of all beams and columns elements in Opensees structural models.

The response spectra of the both components of each record are shown in Fig. 5(a) and 5(b).

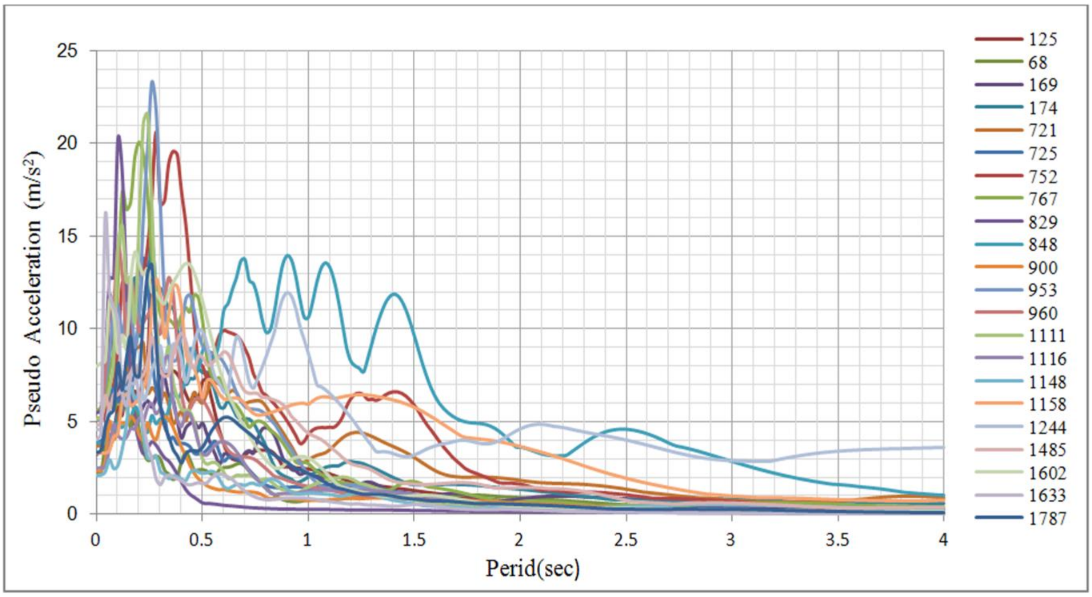

(a) Z Components

Continued

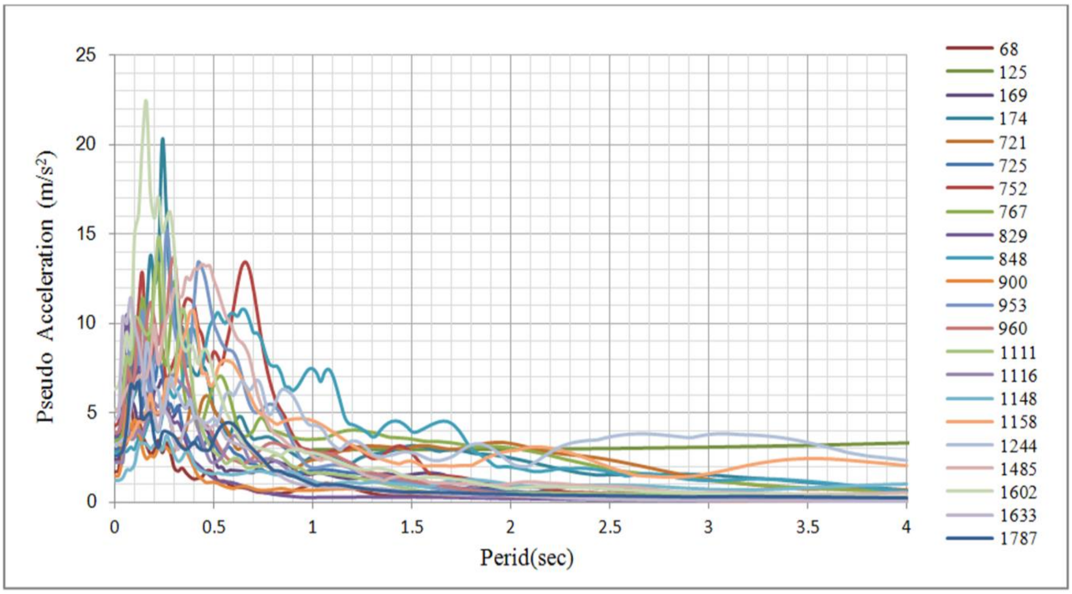

(b) X Components

Fig. 5 Pseudo acceleration spectrum of ground motion records, (a) Z Components and (b) X Components

The PGA level of each of the 22 ground motions is increased by incremental dynamic analysis (IDA) in such a way that after the formation of collapsed hinges, the whole building becomes unstable (FEMA P695, 2009). So, the incremental dynamic analysis is repeated for each record. Therefore, many different seismic hazard levels are adopted for each of 22 ground motion records. Meaning that, not a special seismic hazard level but many seismic hazard levels for each record have been considered.

Here, the results of NLTHA are presented in 2 parts. First, propagations of the progressive collapse are explained and then the relevant story drifts of the symmetric and asymmetric buildings are studied.

3. Collapse propagation

To evaluate the process of collapse propagation, first, symmetric and asymmetric buildings are analyzed due to the earthquake records, and then the sequences of collapsed elements are investigated to evaluate the progressive collapse distributions. In other words, collapse scenarios are tracked in beam and column elements of the buildings and critical elements and significant collapse distributions are identified. Results demonstrate that the most critical elements, and subsequently the propagations of the collapse are the same per each record and mass eccentricity level.

As said before, the aim of this study is the evaluation of the progressive collapse. So, based on the progressive collapse mechanism and the collapse definitions, failure first occurs locally in the structure and then with propagation of the collapse in beam and column elements, one after another, a major portion of the building will fail and finally the structural system becomes unstable. For this reason, the term "collapse propagation" was used in the body of the manuscript.

It should be noted that only those hinges that passed over *Θu* (in Fig. 4) have been shown in the next figures. There are many beam and column hinges that passed over *Θy* and even *Θcap* which can cause general instability of the building. But they have not been shown in the following figures showing collapse distribution.

In Figs. 6 to 19, the first 20 collapsed hinges are demonstrated with different colors in such a way that the darker colors show the hinges which are collapsed in the initial stages of NLTHA. The light colors also show the hinges which are collapsed in the final steps of the NLTHA. In other words, the sequence of collapsed hinges has been demonstrated from the first hinge to the last hinge with a coloring rational which goes from dark to light. Although the numbers illustrate the sequence of collapsed hinges, using the colors is useful to get a rapid visual sense of the collapse tendency in the buildings.

Such a methodology can be used to predict priority of the critical members and spread of the collapse in similar buildings. For example, Figs. 6 to 12 demonstrate the collapse propagations and sequences of the collapsed hinges which are formed in the beam and column elements of the regular and irregular buildings for the earthquake record #752, #1148 and #68. The figures show that the critical hinges and their subsequent critical members are approximately the same in symmetric and asymmetric buildings.

Fig. 6 shows that failure is initiated from the farthest left and right sides (hinges 1, 2, 3, 4, 5 and 6) of the sixth story and after distribution in the central core from outer (hinges 7, 8, 12, and 13) to inner (hinges 9, 11, 14 and 16) perimeter of the core, it finishes in front and back sides of the floor (hinges 15, 16, 19, 20, 21, 22 and 23).

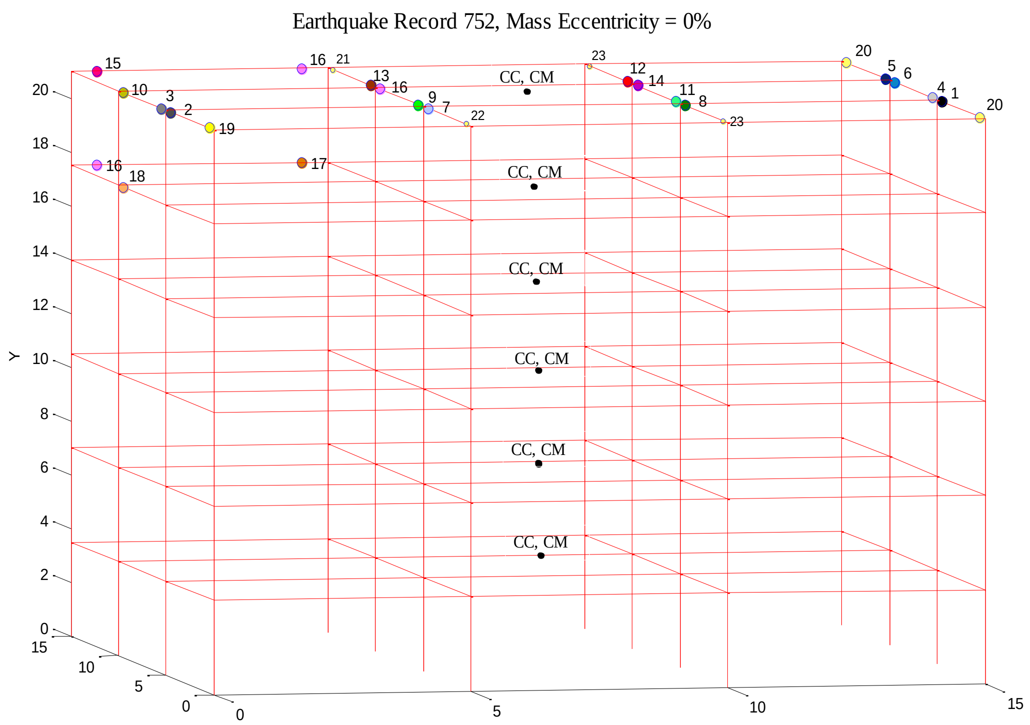

Fig. 6 Collapse distribution in a regular building in presence of the ground motion record #752

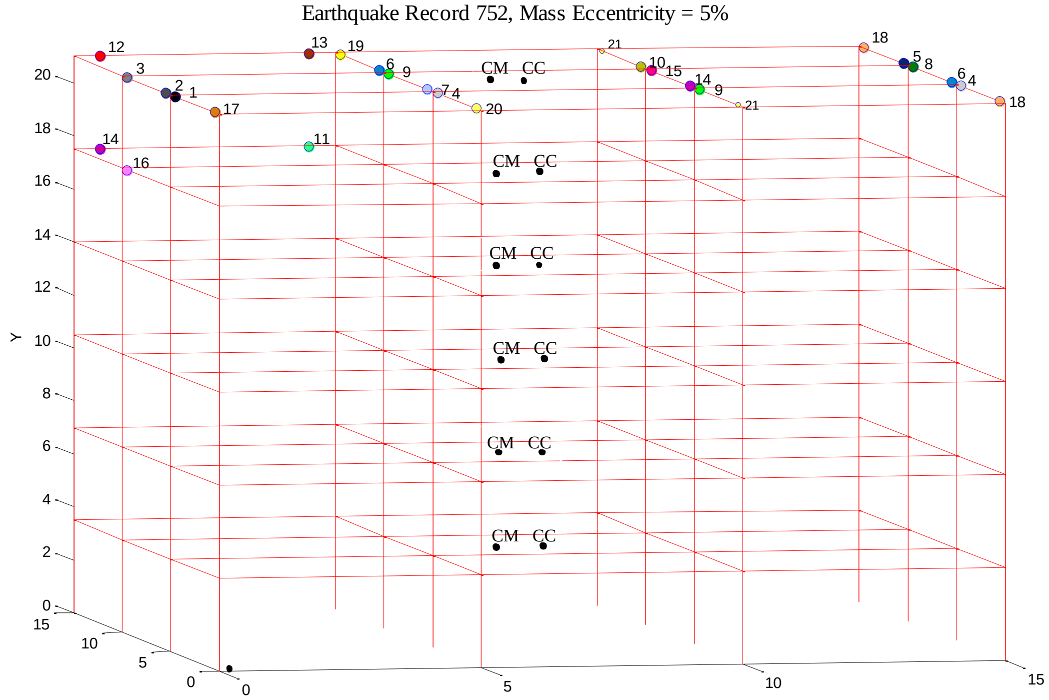

Fig. 7 Collapse distribution in an irregular building with mass asymmetry of 5% in presence of the ground motion record #75

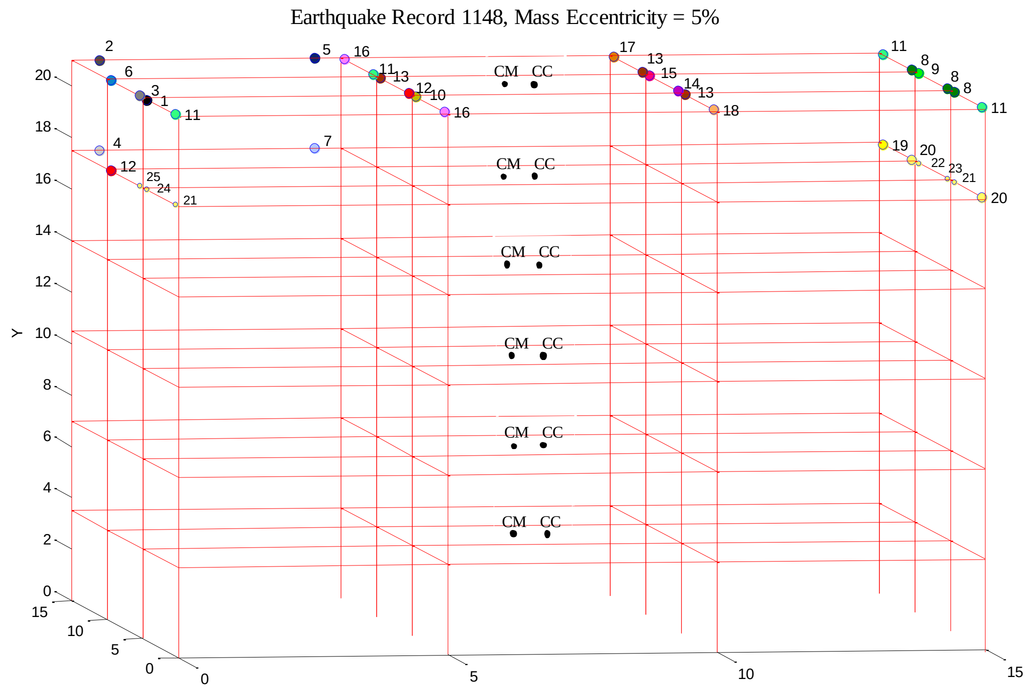

Fig. 8 Collapse distribution in an irregular building with mass asymmetry of 5% in presence of the ground motion record #1148

The collapse propagations in presence of the various ground motion records demonstrate that the collapse distributes in two forms in the building with 5% of mass eccentricity. Figs. 7 and 8 show these two forms of the collapse distribution in presence of the ground motion records #752 and #1148, respectively. According to the Fig. 5, similar to the case of symmetric building, the sixth story starts to collapse from the stiff and flexible edges and after the propagation of collapse in the central core from the outer to inner perimeter of the core, it finishes in front and back sides.

In the second form (See Fig. 8), failure first occurs in the flexible area (hinges 1, 2, 3, 4, 5, 6 and 7), then it distributes in the stiff edge and inner left side frame, simultaneously (hinges 8, 9, 10, 11, 12, 13). Finally, after propagation of the collapse in the inner right side frame (hinges 13, 14 and 15), it will end in front and back frames of the building (hinges 16, 17 and 18).

In the building with 15% of mass asymmetry, the spread of collapse under various ground motion records illustrates that the collapse propagates in two forms, too. Figs. 9 and 10 show how collapse propagates in this type of buildings. According to the Fig. 9, the sixth floor initiates to collapse from the flexible area (hinges 1, 2, 3, 4, 5, 6 and 7) and after the propagation of collapse in the stiff edge (hinges 8 and 9) and then in the inner left side frame (hinges 12, 14 and 15), it will propagate in the inner right side frame (hinges 16, 17, 18 and 19) and finally, it ends up in front and back frames of the floor, simultaneously (hinges 20, 21, 23 and 24).

According to Fig. 10, in the second form of the collapse propagation in the building with 15% of mass asymmetry, flexible edge of the floor starts to collapse from outer frame (hinges 1, 3, 4, 5, 6 and 10) to inner frame (hinges 2, 3, 7, 8 and 9) and after the propagation of collapse in the stiff edge (hinges 11, 12, 13, 14, 18 and 19) it ends up in the inner right side frame (hinges 15,17,18 and 19).

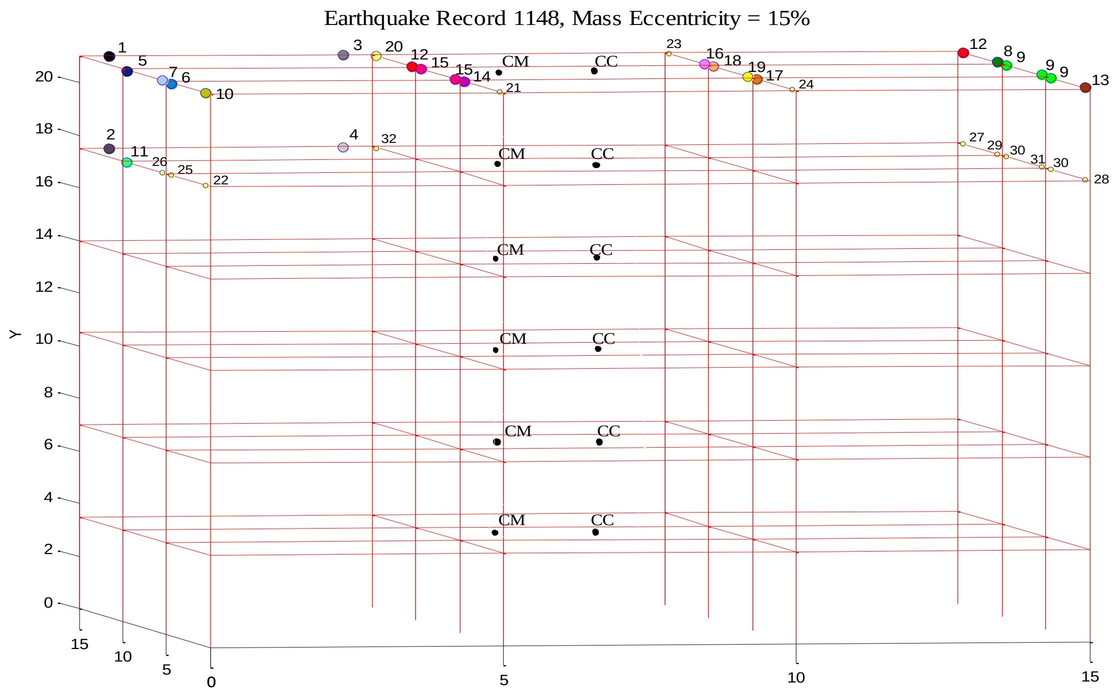

Fig. 9 Collapse distribution in an irregular building with mass asymmetry of 15% in presence of the ground motion record #1148

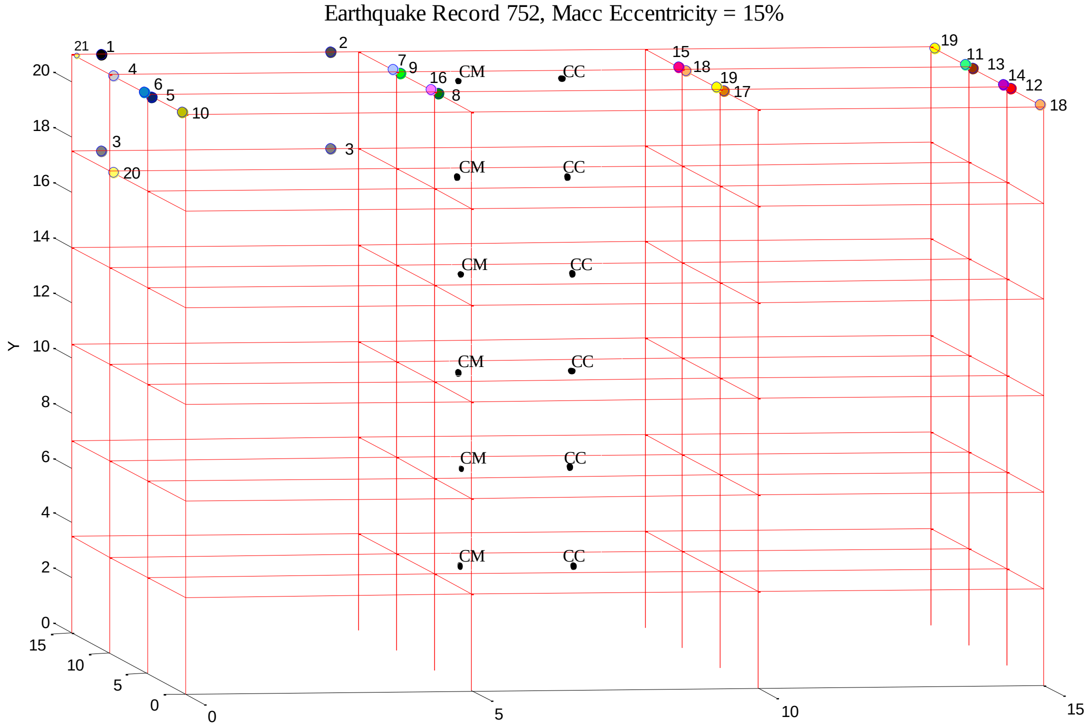

Fig. 10 Collapse distribution in an irregular building with mass asymmetry of 15% in presence of the ground motion record #752

In the building with mass asymmetry of 25%, under some earthquake records, collapse concentrates more in the flexible areas of some floors. Because, mass concentrates more in the flexible areas of those floors. Therefore, unlike other types of the symmetric and asymmetric buildings in which collapse is distributed well in each floor and then is transferred to the other floor, collapse does not propagate in floors one after another, in the presence of some records. Fig. 11 shows collapse propagation in an asymmetric building with mass asymmetry of 25% in presence of the earthquake record # 68.

Also, for other earthquake records in which collapse is distributed completely in one floor after another floor, the spread of collapse is somehow similar to that given by the irregular building with 15% of mass asymmetry. For most of the earthquake records, failure is propagated from the flexible edge to the stiff edge of the building.

The same process has been followed for the other earthquake records and critical collapse hinges have been recognized and the sequence of the collapsed hinges has been determined for the regular and irregular buildings. Results show that the critical collapsed hinges are almost independent of the earthquake records. Such an independency is also held for the collapse propagation pattern in many records. In other words, the first group of critical collapsed hinges and the subsequent critical members are the same in a large number of NLTHA and follow special patterns which are a function of the mass eccentricity levels. Such an outcome sounds promising that it is possible to predict progressive collapse scenarios and collapse propagations of the similar symmetric and asymmetric buildings.

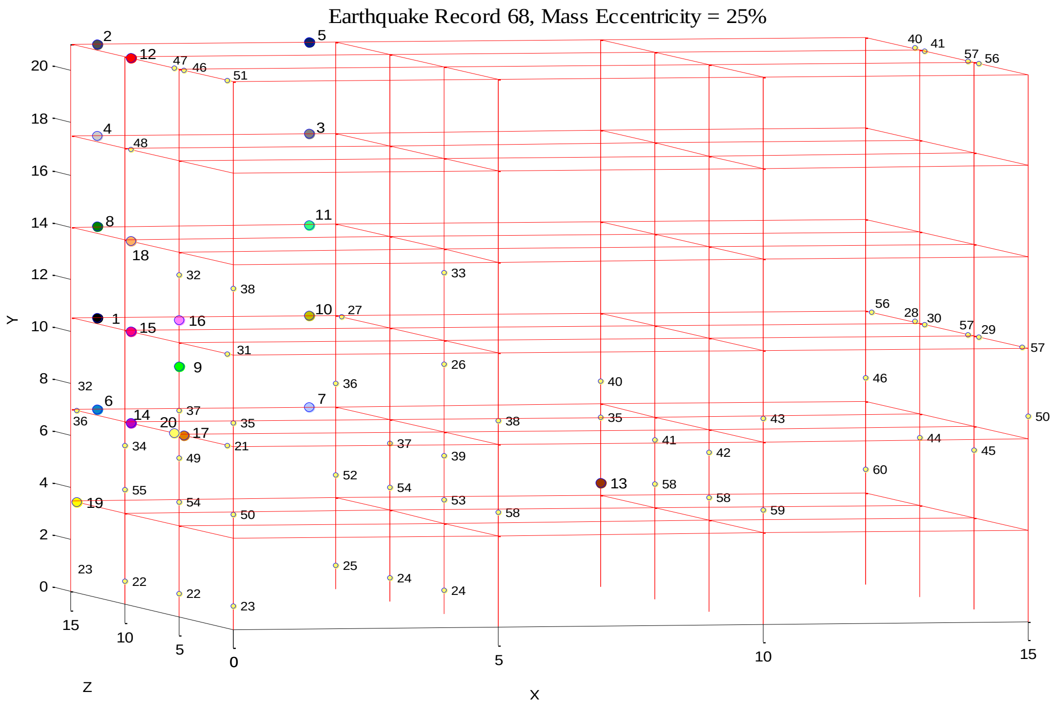

Fig. 11 Collapse distribution in an irregular building with mass asymmetry of 25% in presence of the ground motion record #68

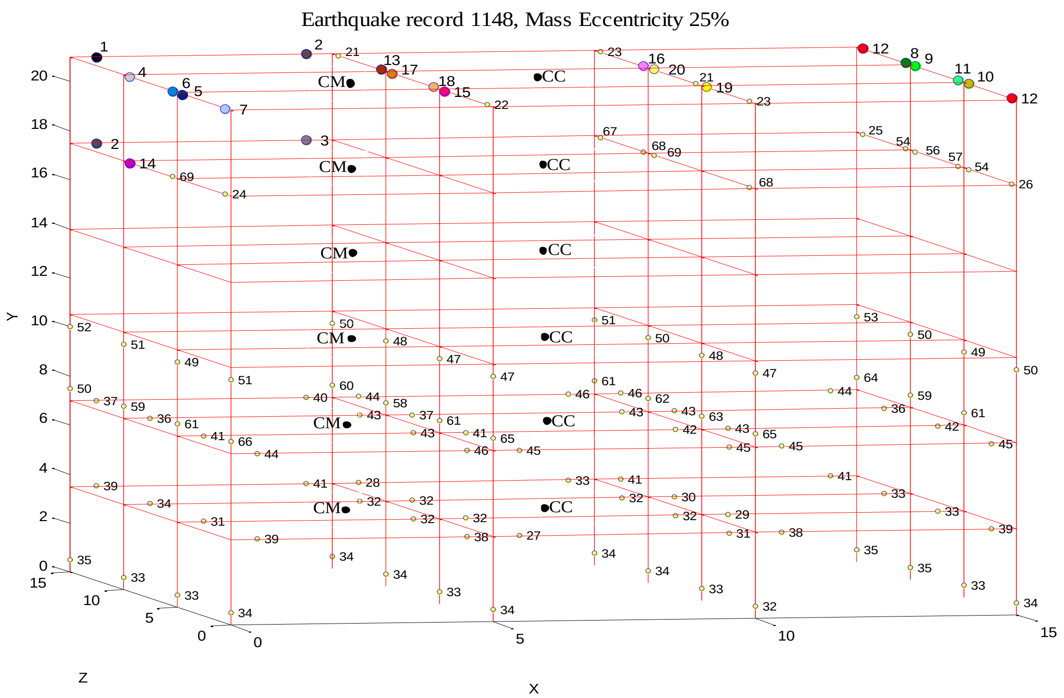

Fig. 12 Collapse distribution in an irregular building with mass asymmetry of 25% in presence of the ground motion record #1148

According to the observations made on different earthquake records, the collapse is distributed in a regular building as follows: first, two edges of the floors fail, simultaneously. Then, the failure continues in the central core of the floors from the outer to inner perimeter and finally it propagates in front and back sides. For example, Fig. 13 demonstrates the collapse propagation in a regular building subjected to the earthquake record #1111.

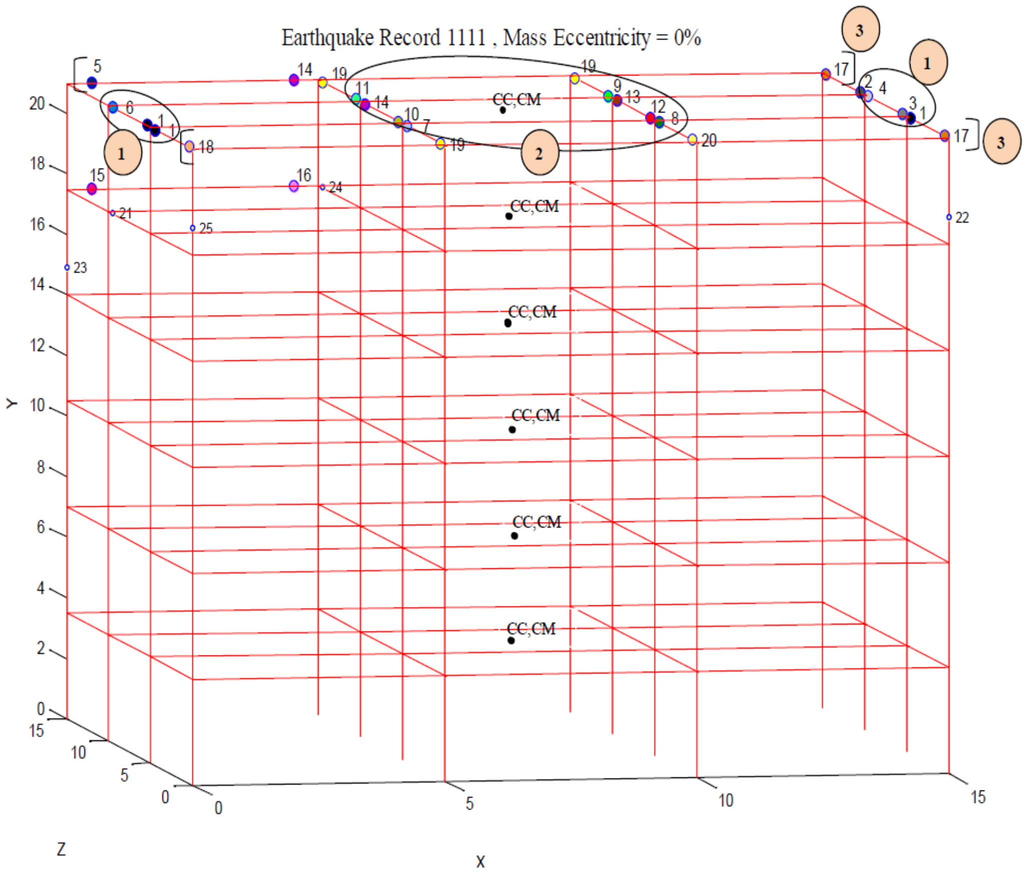

Fig. 13 Collapse distribution in a regular building in presence of the ground motion record #1111

To summarize the collapse distribution in the irregular building with mass asymmetry of the 5%, two patterns of the collapse propagation are observed. Figs. 14 and 15 demonstrate the collapse distribution patterns in an irregular building with mass asymmetry of the 5% subjected to the ground motion record # 68 and #1602, respectively. In the first pattern (See Fig. 14), under some ground motion records, collapse propagation is similar to the regular building. But in the case of irregular building, collapsed hinges concentrate more in flexible areas. In the second pattern (See Fig. 15), at first the flexible edge initiates to collapse, then collapse is distributed in the stiff edge and at the same time in the inner left side frame. Finally, after spread of the collapse in the inner right side frame, it ends up in front and back frames of the floors.

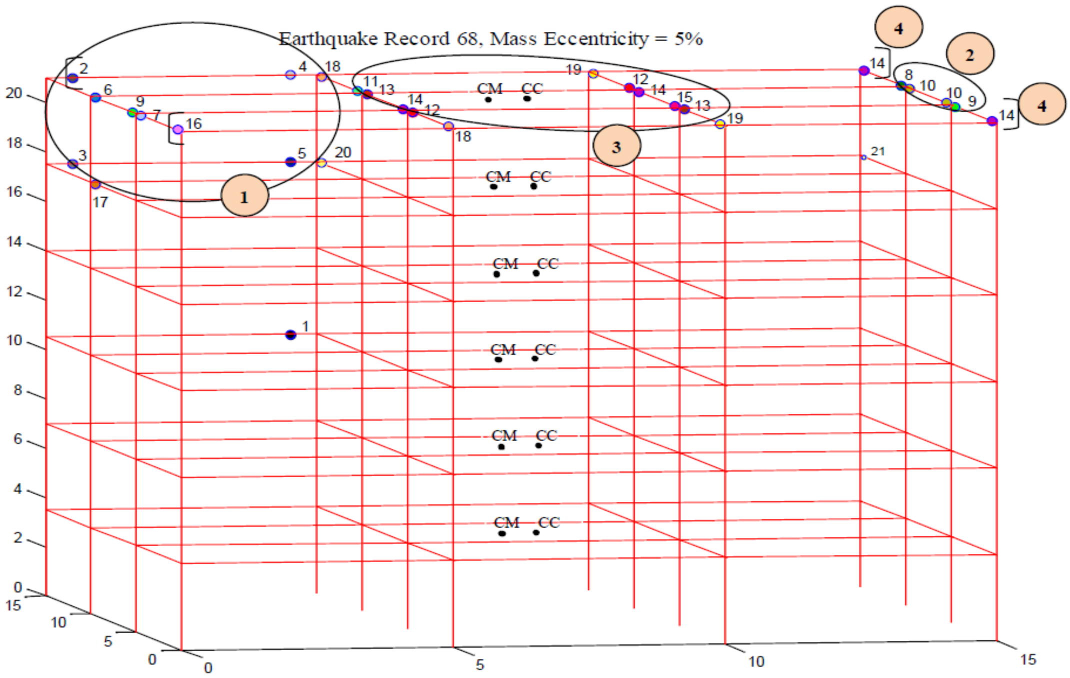

Fig. 14 Collapse distribution in an irregular building with mass asymmetry of 5% in presence of the ground motion record #68

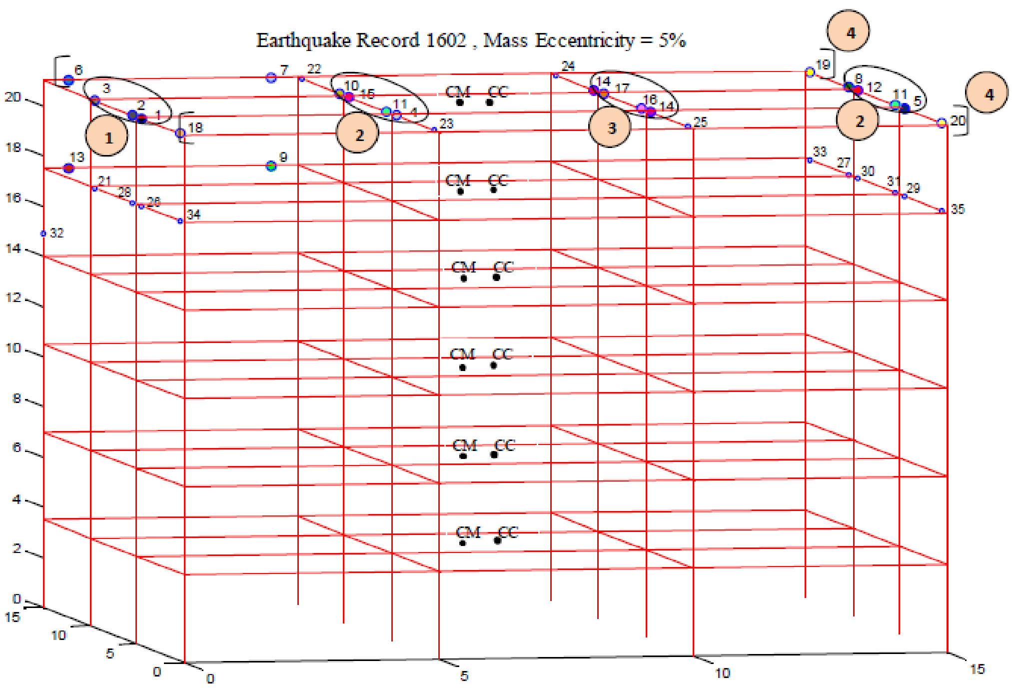

Fig. 15 Collapse distribution in an irregular building with mass asymmetry of 5% in presence of the ground motion record #1602

In the irregular building with mass asymmetry of 15%, collapse propagation starts from the flexible edge. A larger collapse is concentrated in the areas in which a larger mass has been concentrated (i.e., the left side of the building model). In the central core of the floors, collapse

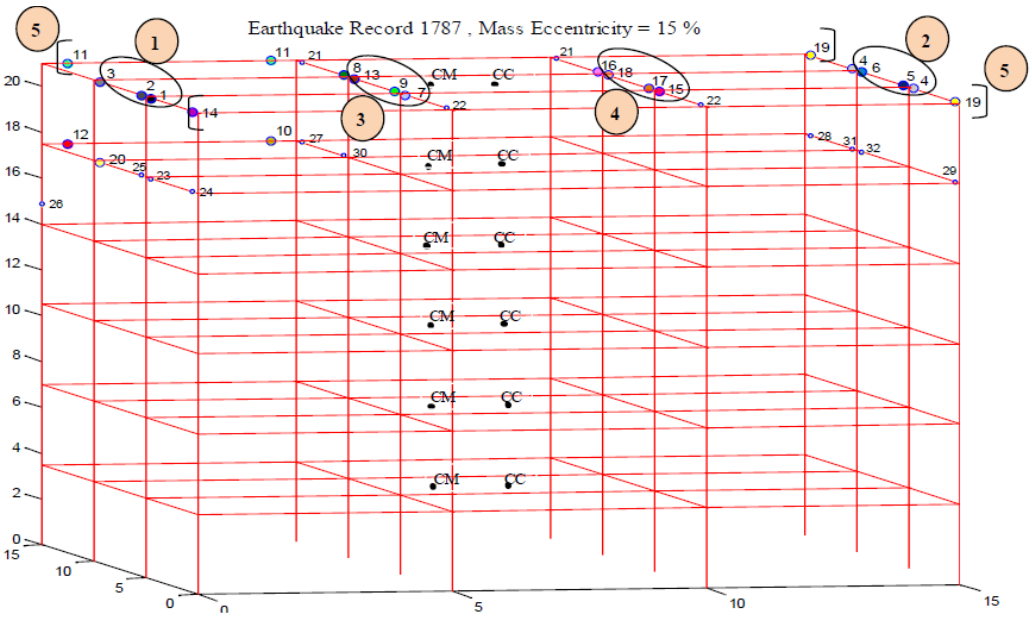

Fig. 16 Collapse distribution in an irregular building with mass asymmetry of 15% in presence of the ground motion record #1787

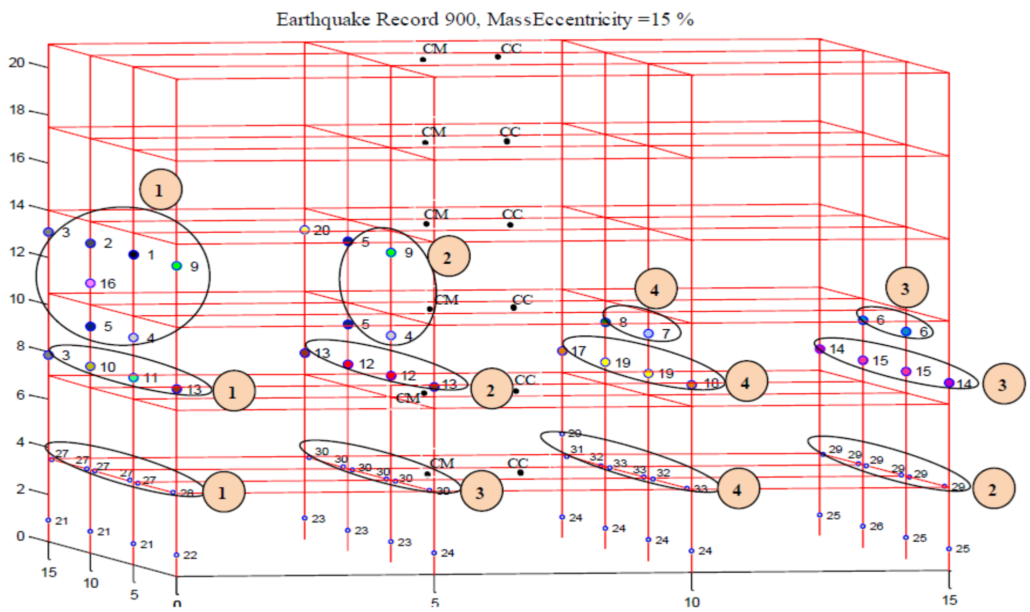

Fig. 17 Collapse distribution in an irregular building with mass asymmetry of 15% in presence of the ground motion record #900

propagates from the outer hinges to inner hinges, too. In this type of buildings, there are two forms of the collapse propagation under different ground motion records. Figs. 16 and 17 demonstrate these two patterns of the collapse distribution in presence of the ground motion record #1787 and #900, respectively.

In the irregular building with 25% of mass asymmetry, collapse propagation under a large number of ground motion records is similar to the building with 15% of mass asymmetry. In this type of buildings, mass is concentrated in the left side of the stories and based on the results, collapse starts from the flexible edge and is concentrated near the mass centers. In other words, the collapse gets concentrated where the mass is concentrated. Collapse distribution in the stories demonstrates that it propagates from the left side to right side of the stories or in other words, collapse distribution is initiated from the flexible edge and is propagated toward the stiff edge, progressively. Fig. 18 illustrates the collapse distribution in an irregular building with mass asymmetry of 25% in presence of the ground motion records #721.

As above figures show, the collapsed hinges were distributed in the top story in most cases. This is enforced by the higher mode effects. Actually, this effect influences on the collapse propagation under several earthquake records. Effective mass is considerable in the higher modes and according to the periods of the buildings structural models shown in Table 1 and the pseudo acceleration spectrum of the ground motion records in Figs. 5(a) and (b), it can be seen that there are many peaks in the pseudo acceleration spectrum of the earthquake records corresponding to the higher mode periods of the buildings. Therefore, such effect intensifies the higher modes effects.

It should be emphasized that, in fact, many beam and column elements severely damaged in the

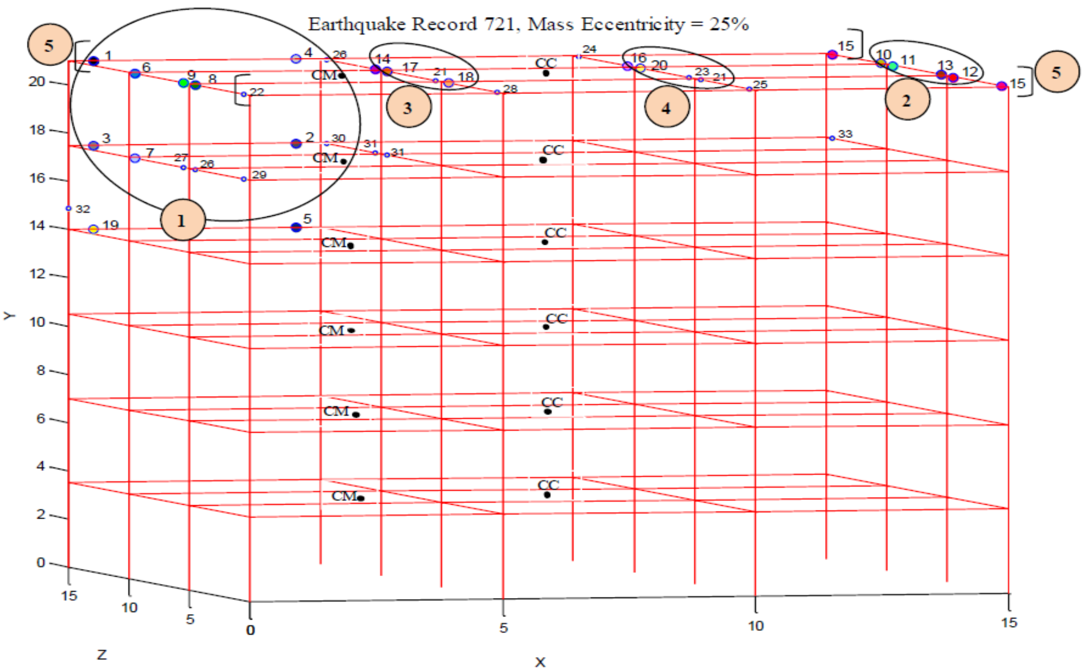

Fig. 18 Collapse distribution in an irregular building with mass asymmetry of 25% in presence of the ground motion record #721

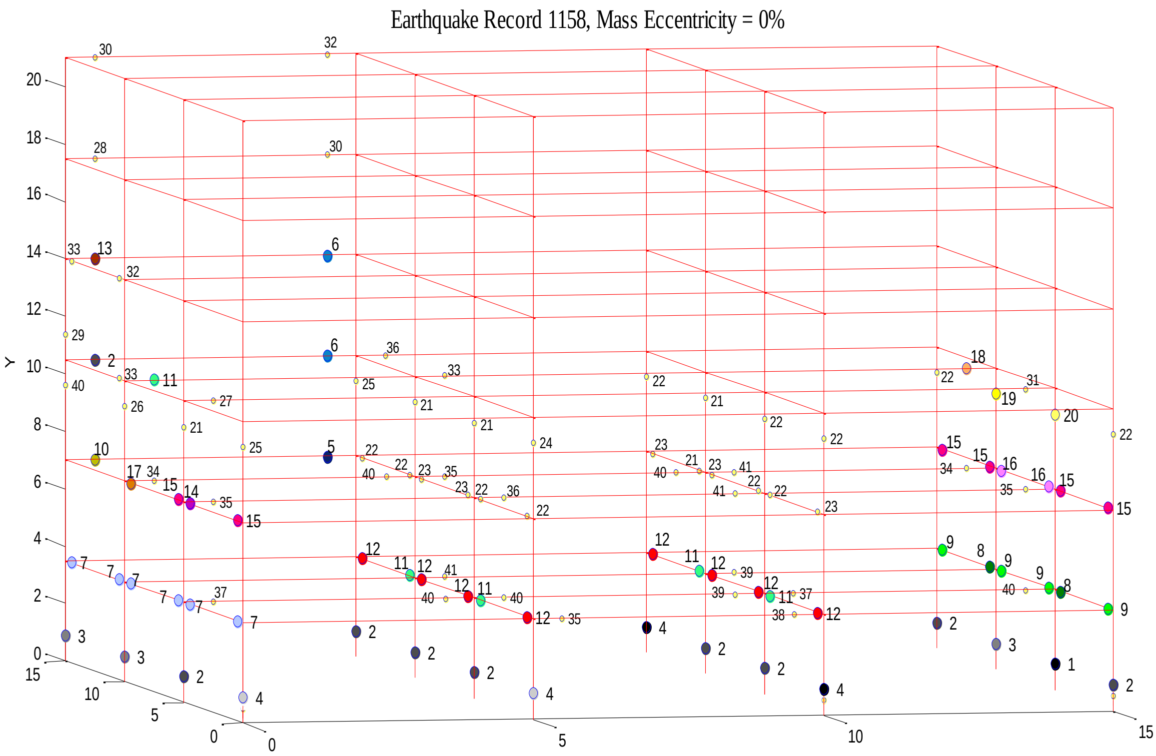

Fig. 19 Collapse propagation in a symmetric building subjected to earthquake record #1158

lower stories. However, the identified hinges illustrated in the figures, are only those damage hinges that passed over the value of *Θu*. Besides, most design codes underestimate the actual "upper stories portion of the lateral loads" (Hajirasouliha and Moghaddam 2009, Hosseini and Khoshahmadi 2008).

With respect to the trends of the collapse distributions in progressive collapse mechanism of the regular and irregular buildings, for 86% of the ground motion records for which collapsed hinges are formed through the 6 stories, it is observed that when the collapse distribution is finished in the outer frames of each story, failure is then initiated in the outer frames of the next story. In a similar way, when the collapse distribution is finished in the inner frames of each story, failure is then initiated in the inner frames of the next story. As an example, Collapse propagation in a symmetric building subjected to the earthquake record #1158 is shown in Fig. 19.

In this study, location of the stiffness centers is in the center of the floors in all buildings. So, when the value of mass eccentricity increases from zero to 25%, mass concentration gets closer to the flexible edges. According to the results, when the mass eccentricity increases, collapse starting point gets closer to the flexible edges, too. In conclusion, collapse initiation points in asymmetric buildings are mostly in the flexible edge areas.

In the majority of the results, the spread of collapse in buildings is horizontal through the stories but not vertical through the height of the buildings, except in buildings with mass eccentricity of 25% in which collapse is distributed vertically in some earthquake records. In most NLTHA, columns contribute in the collapse process in the final steps of the collapse propagation.

4. Story drifts

Since story drifts are among acceptance criteria in various codes and guidelines, one purpose of this study is to achieve acceptable and useful relations between the story drifts by comparing drifts of the mass centers, stiff and flexible edges in the regular and irregular buildings. Consequently, story drifts behavior of the similar buildings can be predicted.

Based on the results of NLTHA, in presence of FEMA P695 ground motion records, the maximum story drifts of mass centers, stiff and flexible edges are compared in symmetric and asymmetric buildings. Figs. 20, 21(a), 22(a) and 23(a) demonstrate the average value of the maximum story drifts of mass centers, stiff and flexible edges in regular and irregular buildings with mass asymmetry of 0%, 5%, 15% and 25%, respectively. Figs. 21(b), 22(b) and 23(b) demonstrate the normalized average values of the maximum story drifts of the mass centers, stiff and flexible edges in the irregular buildings with mass eccentricity of 5%, 15% and 25% with respect to the regular one in presence of 22 earthquake records.

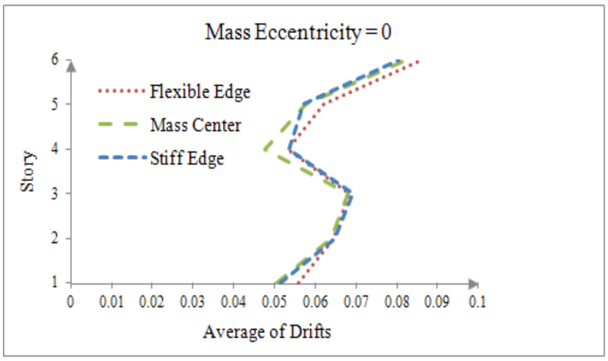

Fig. 20 The average value of maximum story drifts in mass centers, stiff and flexible edges in a regular building in presence of 22 earthquake records

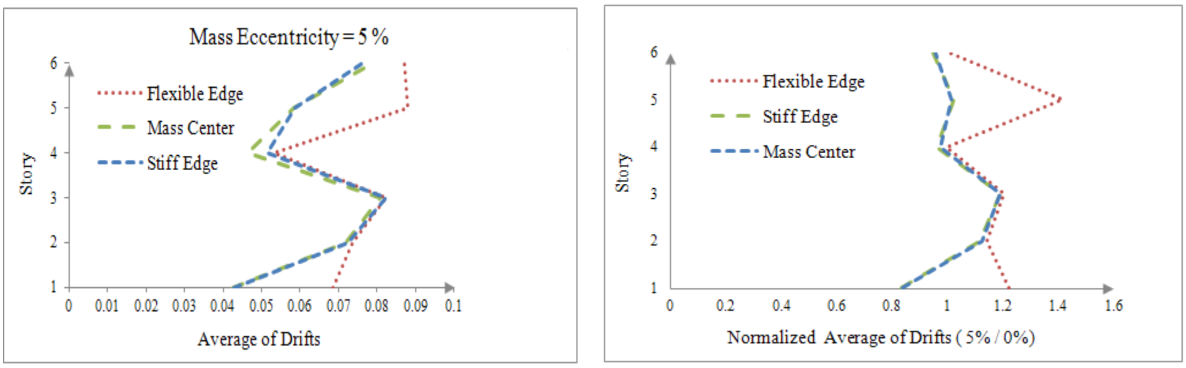

(a) (b)

Fig. 21 (a) The average value of maximum story drifts in mass centers, stiff and flexible edges in an irregular building with mass eccentricity of 5% in presence of 22 earthquake records, (b) The normalized average values of maximum story drifts of the mass centers, stiff and flexible edges in an irregular building with mass eccentricity of 5% with respect to the regular one in presence of 22 earthquake records

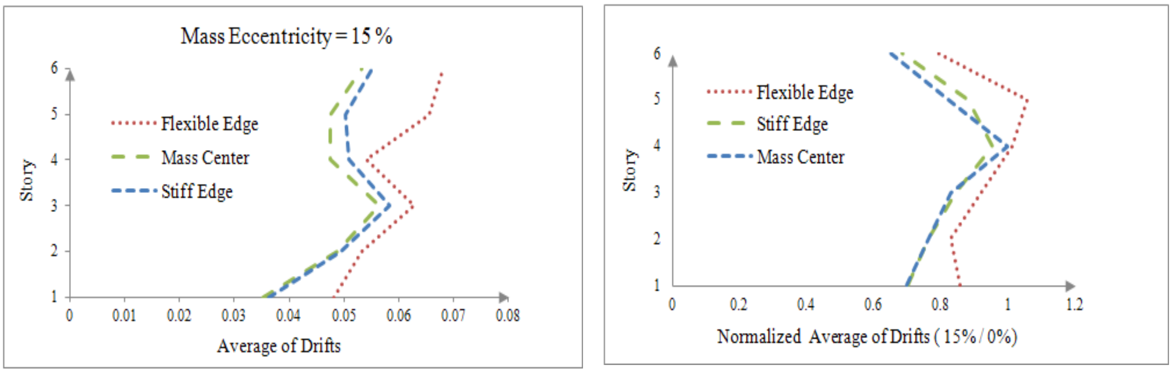

(a) (b)

Fig. 22 (a) The average value of maximum story drifts in mass centers, stiff and flexible edges in an irregular building with mass eccentricity of 15% in presence of 22 earthquake records, (b) The normalized average values of maximum story drifts of the mass centers, stiff and flexible edges in an irregular building with mass eccentricity of 15% with respect to the regular one in presence of 22 earthquake records

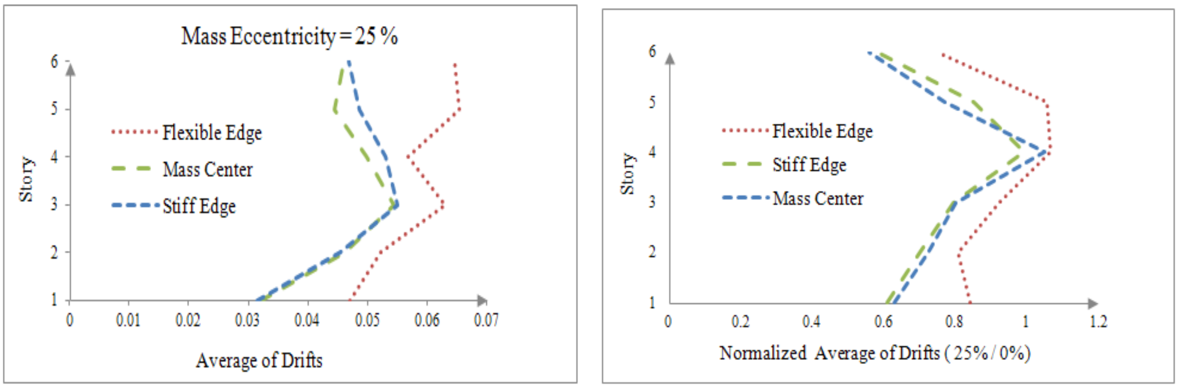

(a) (b)

Fig. 23 (a) The average value of maximum story drifts in mass centers, stiff and flexible edges in an irregular building with mass eccentricity of 25% in presence of 22 earthquake records, (b) The normalized average values of maximum story drifts of the mass centers, stiff and flexible edges in an irregular building with mass eccentricity of 25% with respect to the regular one in presence of 22 earthquake records

As Figs. 20 and 21(a) to 23(a) show, the behavior of the buildings in the mass centers is similar to the stiff edges in 80% of earthquake records and maximum story drifts in the flexible edges are equal or greater than those in the stiff edges and the mass centers.

Figs. 21(b) to 23(b) also show that except for the case of 5% mass eccentricity, story drift values of the irregular buildings are less than the corresponding regular values. Because, increasing the value of mass eccentricity makes the structural system unstable in the lower values of the story drifts. In other words, increasing the mass eccentricity causes an earlier instability and collapse of the irregular buildings, in lower values of inter story drifts, in comparison with the regular one.

A comparison between the main periods of the asymmetric building with the mass eccentricity of 5% in Table 1 and the acceleration response spectra of the ground motion records in Figs. 5(a) and 5(b) shows that the two earthquake records #1148 and #752 have high spectral acceleration values in the main periods of that building. Therefore, there is an increasing trend in the story drift values of the building with the mass eccentricity of 5% in comparison with the regular one.

5. Conclusions

- There are collapse distribution patterns to predict progressive collapse scenarios in beam and columns elements of the regular and irregular buildings.
- Collapse propagation process depends on the level of the mass eccentricity and is independent of the ground motion records.
- In buildings with 0%, 5% and 15% of the mass asymmetry, collapse propagates horizontally through the stories but in buildings with 25% of the mass eccentricity, it propagates vertically through the height of the buildings in presence of the some earthquake records.
- Damage concentrates with a high probability in places with larger mass concentration.
- When the collapse distribution ends in the outer frames of each story, with a high probability (almost 86%) it will initiate again from the outer frames of the next story. In a similar way, when the collapse distribution ends in the inner frames of each story, it initiates again from the inner frames of the next story.
- The flexible edges initiate to collapse with a high probability in irregular buildings.
- For 80% of the results, the story drifts behavior in the mass centers is similar to those given by the stiff edges.

References

Alashker, Y., Li, H. and EL-Tawil, S. (2011), “Approximations in progressive collapse modeling”, *J. Struct. Eng.*, **137**, 914-924.

Bao, Y., Kunnath, S.K., El-Tawil, S. and Lew, H.S. (2012), “Macromodel-based simulation of progressive collapse: RC frame structures”, *Struct. Eng.*, **134**(7), 1079-1091.

Bažant, Z.P. and Verdure, M. (2007), “Mechanics of progressive collapse: learning from world trade center and building demolitions”, *J. Eng. Mech. - ASCE*, **133** (3), 308-319.

Biskinis, D. and Fardis, M.N. (2009), “Deformations of concrete members at yielding and ultimate under monotonic or cyclic loading (including repaired and retrofitted members)”, Report Series in Structural and Earthquake Engineering, Report No. SEE 2009-01.

Burnett, E.F.P. (1975a), “Abnormal loading and building safety”, American Concrete Institute, *Int. Concrete Res. Inform. Portal*, SP **48**, 141-190.

Ellingwood, B. (2006), “Mitigating risk from abnormal loads and progressive collapse”, *J. Perform. Constr. Facil.* **20**, Special Issue: Mitigating the Potential for Progressive Disproportionate Structural Collapse, 315-323.

El-Tawil, S., Khandelwal, K., Kunnath, S. and Lew, H.S. (2007), “Macro models for progressive collapse analysis of steel moment frame buildings”, *Proc. Structures Congress 2007*, Long Beach, CA.

Eslami, A. and Ronagh, H.R. (2012), "Effect of elaborate plastic hinge definition on the pushover analysis of reinforced concrete buildings", *Struct. Des.Tall Sp.*, doi: 10.1002/tal.1035.

Ettouney, M., Smilowitz, R., Tang, M. and Hapij, A. (2012), "Global system considerations for progressive collapse with extensions to other natural and man-made hazards." *J. Perform. Constr. Facil.* **20**, 403-417.

FEMA P695 (2009), *Quantification of building seismic performance factors*, Prepared by Applied Technology Council, www.ATCouncil.org.

Filippou, F.C. (1999), "Analysis platform and member models for performance-based earthquake engineering", *U.S.-Japan Workshop on Performance-Based Earthquake Engineering Methodology for Reinforced Concrete Building Structures*, PEER Report 1999/10, Pacific Earthquake Engineering Research Center, University of California, Berkeley, California, 95-106.

Gurley, C. (2012), "Progressive collapse and earthquake resistance", *Pract. Period. Struct. Des. Constr.-ASCE*, **13**(1), 19-23.

Hafez, I., Khalil, A. and Mourad, S.A. (2013), "Alternate path method analysis of RC structures using applied element method", *Int. J. Protect. Struct.*, Multi-Science Publishing, **4**(1), 45-64.

Hajirasouliha, I. and Moghaddam, H. (2009), "New lateral force distribution for seismic design of structures", *J. Struct. Eng.*, **135**(8), 906-915.

Haselton, C.B. and Deierlein, G.G. (2007), "Assessment seismic collapse safety of modern reinforced concrete moment frame building", John A. Blume Earthquake Engineering Center Technical Report No. 156, Stanford, California.

Haselton, C.B., Liel, A.B., Lange, S.T. and Deierlein, G.G. (2007), "Beam-column element model calibrated for predicting flexural response leading to global collapse of RC frame buildings", PEER Report 2007/03, Pacific Earthquake Engineering Research Center, College of Engineering University of California, Berkeley.

Haselton, C.B., Liel, A.B. and Deierlein, G.G. (2008), "Simulating structural collapse due to earthquakes: model idealization, model calibration, and numerical solution algorithms", *COMPDYN2009, ECCOMAS Thematic Conference on Computational Methods in Structural Dynamics and Earthquake Engineering*, Greece.

Hayes, Jr.J.R., Woodson, S.C., Pekelnicky, R.G., Poland, C.D., Corley, W.G. and Sozen, M. (2012), "Can strengthening for earthquake improve blast and progressive collapse resistance?", *J. Struct. Eng. - ASCE*, **131**(8), 1157-1177.

Helmy, H., Salem, H. and Mourad, S. (2012), "Progressive collapse assessment of framed reinforced concrete structures according to UFC guidelines for alternative path method", *Eng.Struct.*, **42**, 127-141.

Hosseini, M. and Khoshahmadi, A. (2008), "A more realistic lateral load pattern for design of reinforced conceret buildings with moment frames and shear walls", *2008 Seismic Engineering Conference Commemorating the 1908 Messina and Reggio Calabria Earthquake. 2008 American Institute of Physics*, **1**, 955-962.

Ibarra, L.F. and Krawinkler, H. (2004), "Global collapse of deteriorating MDOF systems", *Proc.13thWorld Conference on Earthquake Engineering*, Vancouver, B.C., Canada, August 1-6, Paper No. 116.

Ibarra, L.F. (2005), "Global collapse of frame structures under seismic excitations", Ph.D. thesis, Stanford Univ.

Ibarra, L.F., Medina, R.A. and Krawinkler, H. (2005), "Hysteretic models that incorporate strength and stiffness deterioration", *Earthq. Eng. Struct. Dyn*, **34**, 1489-1511.

Kaewkulchai, G. and Williamson, E.B. (2003), "Beam element formulation and solution procedure for dynamic progressive collapse analysis", *Comp. Struct.*, **82**(7-8), 639-651.

Karbassi, A. and Nollet, M.J. (2013), "Performance-based seismic vulnerability evaluation of masonry buildings using applied element method in a nonlinear dynamic-based analytical procedure", *Earthq. Spectra*, **29**(2), 399-426.

Karimiyan, S., Moghadam, A.S. and Vetr, M.G. (2013), "Seismic progressive collapse assessment of 3-story RC moment resisting buildings with different levels of eccentricity in plan", *Earthq. Struct.*, **5**(3), 277-296.

Khandelwala, K., El-Tawila, S. and Sadekb, F. (2009), "Progressive collapse analysis of seismically designed steel braced frames", *Constr. Steel Res.*, **65**(3), 699-708.

Khandelwal, K., El-Tawil, S., Kunnath, S. and Lew, H.S. (2012), "Macromodel-based simulation of progressive collapse: steel frame structures", *Struct. Eng.*, **134**(7), 1070-1078.

Kim, J. and Hong, S. (2011), "Progressive collapse performance of irregular buildings", *Struct. Des. Tall Sp.*, **20**(6), 721-734.

Kim, J., Choi, H. and Min, K.W. (2011), "Use of rotational friction dampers to enhance seismic and progressive collapse resisting capacity of structures", *Struct. Des. Tall Sp.*, **20**(4), 515-537.

Krawinkler, H., Zareian, F., Lignos, D.G. and Ibarra, L.F. (2009), "Prediction of collapse of structures under earthquake excitations", *COMPDYN 2009, ECCOMAS Thematic Conference on Computational Methods in Structural Dynamics and Earthquake Engineering*, Greece.

Lew, H.S. (2003), *Best practices guidelines for mitigation of building progressive collapse*, National Institute of Standards and Technology, Gaithersburg, Maryland, U.S.A, 20899-8611, hsl@nist.gov.

Li, Y., Lu, X.Z., Guan, H. and Ye, L.P. (2011), "An improved tie force method for progressive collapse resistance design of reinforced concrete frame structures", *Eng. Struct.*, **33**(10), 2931-2942.

Lignos, D.G., Zareian, F. and Krawinkler, H. (2008), "Reliability of a 4-story steel moment-resisting frame against collapse due to seismic excitations", *ASCE Structures Congress*, 1-10.

Lignos, D. and Krawinkler, H. (2012), "Sidesway collapse of deteriorating structural systems under seismic excitations", The John A. Blume Earthquake Engineering Center, Stanford University.

Lignos, D. and Krawinkler, H. (2013), "Development and utilization of structural component databases for performance-based earthquake engineering", *J. Struct. Eng.*, **139**, Special Issue: Nees 2: Advances in Earthquake Engineering, 1382-1394.

Lu, X.Z., Lin, X., Ma, Y., Li, Y. and Ye, L. (2008), "Numerical simulation for the progressive collapse of concrete building due to earthquake", *Proc. the 14th World Conference on Earthquake Engineering*, Beijing, China.

Lu, X.Z., Li, Y., Ye, L.P., Ma, Y.F. and Liang, Y. (2008), "Study on the design methods to resist progressive collapse for building structures", *Proc. Tenth Int. Symp. On Structural Engineering for Young Experts*, 478-483.

Lu, X., Lu, X., Guan, H. and Ye, L. (2013), "Collapse simulation of RC high-rise building induced by extreme earthquakes", *Earthq. Eng. Struct. Dyn.*, **42**(5), 705-723.

Li, Y., Lu, X.Z. and Ye, L.P. (2011), "Study on the progressive collapse mechanism of RC frame structures", *Build. Sci.*, **27**(5), 12-18.

Masoero, E., Wittel, F., Herrmann, H. and Chiaia, B. (2010), "Progressive collapse mechanisms of brittle and ductile framed structures", *J. Eng. Mech*., **136**(8), 987-995.

Nateghi-A, F. and Parsaeifard, N. (2013), "Studying the effect of initial damage on failure probability of one story steel buildings", *Iran. J. Energ. Environ.*, **4**(3), 258-264.

Orton, S. and Kirby, J. (2013), "Dynamic response of a RC frame under column removal", *J. Perform. Constr. Facil*., 10.1061/(ASCE)CF.1943-5509.0000464.

Panagiotakos, T.B. and Fardis, M.N. (2009), "Deformations of reinforced concrete members at yielding and ultimate", *Struct. J.*, **98**(2), 135-148.

Pekau, O.A. and Cui, Y. (2005), "Progressive collapse simulation of precast panel shear walls during earthquakes", *Comput. Struct.*, **84(**5-6), 400-412.

Sasani, M., Bazan, M. and Sagiroglu, S. (2007), "Experimental and analytical progressive collapse evaluation of an actual RC structure", *Struct. J.*, **104**(6), 731-739.

Sasani, M. and Kropelnicki, J. (2008), "Progressive collapse analysis of an RC structure", *Struct. Des. Tall Sp.*, **17**(4), 757-771.

Sasani, M. and Sagiroglu, S. (2008), "Progressive collapse resistance of hotel San Diego", *J. Struct. Eng.*, **134**(3), 478-488.

Sasani, M. and Sagiroglu, S. (2008), "Progressive collapse of RC structures: a multihazard perspective", *Struct. J.*, **105**(1), 96-103.

Somes, N.F. (1973), "Abnormal loading on buildings and progressive collapse", in Building Practices for Disaster Mitigation (Wright, Kramer and Culver, eds.), *Build. Sci.*, Series No. 46, National Bureau of Standards, Washington, DC.

Stinger, S. and Orton, S. (2013), “Experimental evaluation of disproportionate collapse resistance in RC frames”, *ACI Struct. J.*, **110**(3), 521.
Talaat, M. and Mosalam, K.M. (2009), “Modeling progressive collapse in reinforced concrete buildings using direct element removal”, *Earthq. Eng. Struct. Dyn*., **38**, 609-634.
Tsai, M.H. and Lin, B.H. (2008),“Investigation of progressive collapse resistance and inelastic response for an earthquake-resistant RC building subjected to column failure”, *J. Eng. Struct.*, **30**(12), 3619-3628.
Zareian, F., Lignos, D.G. and Krawinkler, H. (2009), “Quantification of modeling uncertainties for collapse assessment of structural systems under seismic excitations”, *COMPDYN 2009*, *ECCOMAS Thematic Conference on*, *Computational Methods in Structural Dynamics and Earthquake Engineering*, Greece.
Zareian, F. and Medina, R.A. (2010), “A practical method for proper modeling of structural damping in inelastic plane structural systems”, *J. Comput. Struct.*, **88**, 45-53.

IT

Appendix: the list of notations

δc = cap deformation (deformation associated with Fc for monotonic loading)
Fy = effective yield strength, incorporating "average" strain hardening
Δy = effective yield deformation (= Fy/Ke)
Ke = effective elastic stiffness
Fr = residual strength capacity
δr = deformation at residual strength
δu = ultimate deformation capacity
δp = plastic deformation capacity associated with monotonic loading
δpc = post-capping deformation capacity associated with monotonic loading
Fc/Fy = post-yield strength ratio
Fyp = predicted effective yield strength (predicted from measured material properties)
Fyn = nominal effective yield strength (predicted from nominal material properties)
κ = residual strength ratio = Fr/Fy
Strain hardening ratio $\alpha s = Ks/Ke = [(Fc/Fy)/\delta p]/Ke$
Post-capping stiffness ratio $\alpha c = Kpc/Ke = (Fc/\delta pc)/Ke$
Fc = strength cap (maximum strength, incorporating "average" strain hardening)
My = yield moment for Ibarra material model (nominal moment capacity of the column)
Mc = moment capacity at the capping point; used for prediction of hardening stiffness
Kc = post-capping stiffness, i.e., stiffness beyond Θcap, pl
Ke = effective elastic secant stiffness to the yield point
Ks = hardening stiffness, i.e., stiffness between Θy and Θcap, pl
Θy = chord rotation at yielding, taken as the sum of flexural, shear and bond-slip components; yielding is defined as the point of significant stiffness change, i.e., steel yielding or concrete crushing (radians)
Θcap = Θcap^{tot} = total chord rotation at capping, sum of elastic and plastic deformations (radians)
Θcap^{p} (Or Θp) = plastic chord rotation from yield to cap (radians)
Θp = plastic chord rotation from yield to cap (radians)
Θpc = post-capping plastic rotation capacity, from the cap to point of zero strength (radians)
Θu = $\Theta y + \Theta p + \Theta pc$